Journal of Applied Fluid Mechanics, Vol. 10, No. 1, pp. 31-40, 2017.
Available online at www.jafmonline.net, ISSN 1735-3572, EISSN 1735-3645.
DOI: 10.18869/acadpub.jafm.73.238.25638

Acoustic Detection of Cavitation Inception

M. A. Hosien† and S. M. Selim

Mechanical Power Engineering Department, Faculty of Engineering, Menoufyia University, Shebin El-Kom Egypt

†*Corresponding Author Email: mohamed_abdelaziz14@yahoo.com*

(Received September 22, 2015; accepted July 15, 2016)

ABSTRACT

Cavitation phenomenon can cause deterioration of the hydraulic performance, damage by pitting, material erosion, structure vibration and noise in fluid machinery, turbo-machinery, ship propellers and in many other applications. Therefore, it is important to detect inception of cavitation phenomenon. An experimental study has been carried out in order to investigate the noise radiated by various cavitating sources to determine the validity of noise measurements for detecting the onset of cavitation. Measurements have been made measuring the noise radiated by a number of configurations in a water tunnel at various operating condition to determine the onset of cavitation. The measurements have been conducted over a frequency range of 31.5 Hz to 31.5 kHz in one-third octave bands. The onset of cavitation was measured visually through a Perspex side of the working section of the water tunnel. Moreover, a theoretical estimate of the pressure radiated from the cavitation nuclei at their critical radii and their frequency was presented. Tests indicated that, generally, at the point of visual inception there was a marked rise of the sound pressure level in the high-frequency noise, whilst the low-frequency noise increased as the cavitation developed. This finding was supported by the theoretical estimate of the pulsating frequency of cavitation nuclei. The results illustrated that the visual observations of inception confirm the noise measurements.

Keywords: Cavitation; Noise; Sound pressure level; Acoustic.

NOMENCLATURE

N	the number of bubbles collapsing per unit time	R	bubble radius
P	pressure	t	collapse time.
p_v	vapor pressure at given tunnel water temperature	σ_{ob}	value of σ_o when the breakdown condition has been reached
P_0, U_0	pressure and velocity upstream of the cavitating source in the working section of the water tunnel.	σ_{oi}	Inception Cavitation number

1. INTRODUCTION

It is well known that cavitation causes lowering performance and efficiency physical damage and associated with noise and vibration. Noise being a basic consequence of cavitation can be used as an indicator of inception of cavitation.

There is a few different methods for cavitation monitoring that can be used to prevent destructive consequences of cavitation in the hydraulic systems, Chudina (2003).

Acoustic methods of detecting cavitation have been used sometime in physical and naval applications, Moussatov *et al.* (2005). They conducted theoretical and experimental analysis of the ultrasonic cavitation generated in a thin liquid layer trapped between a sonotrode surface and a reflector. It has been found that this configuration leads to a large amplification of the acoustic pressure which makes the generation of cavitation possible at low power or in a wide frequency range.

They found that two types of cavitation were observed in the liquid layer, a stable bubble structure is formed on the symmetry axis and transient unstable bubble structures appear at several locations of the surface. These structures are similar to those observed by, Moussatov *et al.* (2003-a). Their generation is associated with the appearance of a strong nonlinear acoustic field in

the liquid, Moussatov *et al.* (2003-b) and Campos-Pozuelo *et al.* (2005). Cheolsoo Park *et al*. (2009), proposed a propeller noise localization method in a cavitation tunnel. They concluded that the proposed method could be a useful tool for various applications including the acoustical detection of cavitation inception.

Jensen and Dayton (2000), conducted experimental measurements of cavitation audible and inaudible sound. Their measurements revealed interesting result during cavitation testing. In addition they observed that the audible noise of the pump decreased upon onset of cavitation.

Alfayez and Mba (2004) investigated the application of acoustic emission (AE) for detecting incipient cavitation. Their results demonstrated that the successful use of the AE technique for detecting incipient cavitation. Furthermore, they indicated that the AE technique can clearly identify the best efficiency point for a system employing pumps.

Alhasmi (2005), took the first steps in processing vibration signals from a centrifugal pump in an attempt to detect the onset of cavitation. He performed the standard time-domain analyses such as RMS and frequency spectrum but he also used probability density function and standard deviation for analyzing the acquired data in the time-domain. He introduced two new possible methods for the detection of cavitation; the measurement of the instantaneous speed of rotation of the pump shaft and analysis of the electric current through the motor driving the pump.

Franc (2006) presented the basic concepts and tools required to understand the inception and development of cavitation in liquid flows. The influence of various parameters as the boundary layer and nuclei content were discussed. A special attention is given to thermal effects which may significantly influence the development of cavitation in thermosensitive fluids as cryogenic liquids. The main types of cavitation (partial attached cavities, travelling bubble cavitation, vortex cavitation and shear cavitation) were presented.

Cernetic *et al.* (2008) performed experimental work using signals of vibration and noise which used for detection and monitoring of cavitation in kinetic pumps. Their experimental results indicated that when cavitation is fully developed, the measured signals at a characteristics frequency or range of frequencies start decrease. Also, they performed a comparison between theoretical expectation and measurement results. The comparison showed a good agreement between them. Also they investigated cavitation detection by monitoring noise and vibrations, both measured outside of two centrifugal pumps and in a frequency band between 20 Hz and 20 kHz. Despite many losses in signal transfer between a source and a microphone or an accelerometer, it is possible to determine the onset of cavitation in a pump.

Čudina and Prezelj (2009) compared airborne, vibration and acoustic emission (AE) methods for the detection of cavitation and concluded, surprisingly, that the latter two offer fewer opportunities than airborne acoustic methods. They suggested that visualization is suitable for high powered pumps and water turbines but cite no examples of its industrial use.

Wu *et al.* (2010) carried out an experimental study in order to analyze the cavitation of a centrifugal pump and its effect on transient hydrodynamic performance during transient operation. Their results showed that the dynamic performance of the centrifugal pump was related to the cavitation of the pump during the low suction pressure starting period.

Al Thobiani *et al.* (2011) reported the results of experiments to predict the onset of cavitation using a range of statistical parameters derived from: the vibration signal obtained from an accelerometer on the pump casing. The airborne acoustic signal from a microphone close to the outlet of the pump and the waterborne acoustic signal from a hydrophone in the outlet pipe close to the pump were recorded. An assessment of the relative merits of the three methods for the detection of incipient cavitation is given based on a systematic investigation of a range of statistical parameters from time and frequency domain analysis of the signals.

Čudina (2012) presented experimental work used audible sound for monitoring cavitation in a pump. He reported that there was a discrete frequency tone or narrowband frequency range within the audible noise spectra, which are in strong correlation with development of the cavitation process in the pump. The results showed that the amplitudes in the narrowband frequency range are increased by up to 15 dB (A) and more when cavitation is fully developed. He concluded that, this characteristic discrete frequency tone or narrowband frequency range can be used to detect the incipient of cavitation and its development.

Černetič and Čudina (2012) examined some important phenomena regarding cavitation noise in centrifugal pumps in audible frequency range. When the cavitation is increasing, the emitted noise in the surroundings increases. They showed that the cavitation noise characteristics can be successfully used for detecting onset and development of cavitation in centrifugal pumps.

Alhashmi (2013) presented non-destructive method to detect and diagnose cavitation in centrifugal pumps using statistical analysis of acoustics signals. The acoustics data was measured close to the discharge port and analyzed in the time domain. It was found that the probability density function (PDF) and standard deviation (SD) values of pump noise can be used successfully for detecting cavitation in centrifugal pump.

Gupta *et al.* (2013) Performed experimental study on a centrifugal pump at different capacities to analyze the level of sound due to cavitation and the change in the level of sound with the change in discharge level. Different parameters related to sound has also been measured. The different

calculations based on sound have been performed to analyze the result. These results help to develop an online detection technique for centrifugal pump using audible sound.

Mostafa *et al.* (2016) presented a numerical study of unsteady behavior of cavitating flow on hydrofoils using bubble dynamics cavitation model. The study focuses on cavitation inception, the shape and general behavior of sheet cavitation. Analysis was done for different cavitation numbers and the computed maximum cavity length and maximum cavity thickness showed good correlation with cavitation numbers.

Based on the previous literature review and importance to detect the onset of cavitation in various hydraulic machines, a more study is required to establish using of acoustic measurements to detect cavitation inception. Therefore, the aim of the present paper is to use noise technique to detect when cavitation occurred for different cavitation configurations, with a view to assessing the onset of cavitation in a prototype machine by measuring the sound pressure level.

2. NOISE GENERATED BY SPHERICAL CAVITY BUBBLE AT INCIPIENT STAGE

Many of fluid mechanics and acoustics exhibit spherical symmetry and are better treated in spherical coordinate. It is assumed that during the entire period of inception, the bubble remain spherical. In spherical coordinate r, θ, φ, the pressure is independent of the coordinates θ and φ owing to the spherical flow symmetry.

The acoustic radiated pressure at the distance r from the center of spherical cavity nuclei is given by the following expression,

$$\underline{\overset{/}{p}}(r) = i\frac{\omega Q}{4\pi r}e^{i(\omega t - kr)} \tag{1}$$

Details of the derivation of Eq. 1. are shown in Appendix A.

Previous results of the static and dynamics testes on the tensile stresses of water at which cavitation occurs showed that the recorded strength of pure water was always far less than the physical tensile strength of pure water. This means that discontinuities in ordinary unpurified water occur at weak points. The gas nucleus in the liquid acts as a weak point in the liquid. When a viscous liquid flows past a solid surface pulsating velocity components and associated pulsating pressure increments appear in turbulent boundary layer or liquid shear layer. Thus, incipient microscopic cavitation bubbles are expected to appear first within the thin boundary layer or at the actual surface of the body. Thus, the microscopic bubbles grow rapidly when they reach their critical size at which the minimum equilibrium pressure in the liquid is obtained.

The conditions for static equilibrium of tiny bubbles filled with water vapors and a certain amount of gas diffusing slowly within the bubble from the surrounding water can be written as:

$$p = p_v + p_g - 2s/r \tag{2}$$

Where p, p_v and p_g are the pressures of the water surrounding the bubbles, saturated vapor at bulk water temperature, and gas pressure within the bubble. S is the surface tension of water (0.0726 N/m). r is the radius of the bubble. It is assumed that the pressure of the water vapors filling the bubble is constant while the gas pressure varies isothermally. Thus the gas pressure can be represented as:

$$p_g = \left(p_0 - p_v + \frac{2s}{r_0}\right)\left(\frac{r_0}{r}\right)^3 \tag{3}$$

The subscript "0" refers to the initial values of the appropriate quantity.

Substituting Eq. 2. into 3., and then differentiating the resultant equation with respect to r and setting the derivative equals to zero, the critical radius (r_{cr}) of the bubble is expressed by the following equation:

$$r_{cr} = \sqrt{3}r_0\sqrt{\frac{r_0}{2s}}\left(p_0 - p_v + \frac{2s}{r_0}\right) \tag{4}$$

Therefore, a cavitation bubble nuclei whose initial radius is r_0 at initial ambient pressure p_0 will grow and pass a critical radius when the pressure at the surface of the bubble falls below the critical pressure, i.e., $\underline{\overset{/}{p}}(r) \prec p_{cr}$. Accordingly, the number of nuclei which will grow should depend on the distribution of nuclei in size and number, and critical radius of nucleus under given flow conditions. Keller (1971) developed an optical measuring method for determining the nuclei spectrum. His measurements encompass a range of nucleus radii from 3.5 μm to 8.6 μm; nuclei with a radius lager than 8.6 μm were summed up.

From Eqs. (1) and (4) it is possible to show the variation of the critical nuclei radius (r_{cr}), the pressure at the nuclei surface ($\underline{\overset{/}{p}}(r)$) and the pulsating frequency (f) of the nuclei as function of the initial nuclei radius (r_0) from 3 μm to 10 μm at water external pressure to the nuclei surface of 9.81 kPa and a bulk water temperature of 26 ˚C. These variations are shown in Fig. 1. It can be seen from Fig. 1 that as the initial radius of the cavitation nuclei (r_0), increases the critical cavitation nuclei radius (r_{cr}) increases too. In Fig. 1. both the pressure at nuclei surface inside the bubble $\underline{\overset{/}{p}}(r_{cr})$, and the pulsating frequency of the nuclei decrease rapidly with increasing of the initial nuclei radius (r_0) in the region between

approximately 3 μm and 10 μm. The values of pulsating frequency of the nuclei at incipient cavitation ranged from 4 Hz up to 3 kHz for a range of initial bubble radii from 10 μm to 3 μm, respectively.

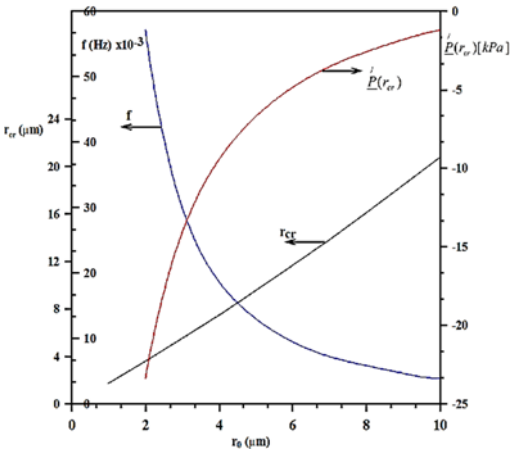

Fig. 1. Variation of critical cavitation nuclei radius (r_{cr}), critical pressure at the nuclei surface ($\overline{p'(r_{cr})}$), and the frequency (f) of the liquid contains gas nuclei with various initial nuclei radii (r_0).

3. EXPERIMENTAL WORKS

The experiments were conducted in a variable pressure closed circuit water tunnel. The tunnel consists of two working sections, one with a cross section 40x20 mm and the other 20x10 mm. The front of test section is provided with a transparent Perspex cover to permit visual and photographic studies. The water was circulated by a 20 kW centrifugal pump and bypass control to give velocities ranging from 20- 40 m/sec at the throat of the cavitation source. The rig could be pressurized and controlled from 0—10 bar by a pressure regulation chamber supplied with air from a compressor. The main components of the test rig are shown in Fig. 2. The average temperature of the test water was kept within 32 ± 2 °C by cooling coils which were supplied by water from a laboratory tap.

The configurations for inducing cavitation were con-div. wedge, rear facing step and forward facing step, and for each configuration two sizes, 20 mm and 10 mm, were used. The blockage ratio for 20 mm and 10 mm sources was the same and equal to 0.5. The con-div. wedge is intended to simulate the type of impeller blades where the leading edge of the blade corresponds to the sharp edge at the throat. The rear facing step and the forward facing step are similar to the type of cavitation occurring in the flow through a valve and the flow through a sudden constriction, respectively. Details of the configurations are shown in Fig. 3.

4. TECHNIQUES AND TEST PROCEDURE

4.1 Noise Measurements

Measurements of pressure produced by cavitation have been obtained by a vibrometer quartz piezo electric transducer (type 6Qp 500) of diameter 6 mm which was flush mounted in the working section of the tunnel. It was placed about 215 mm and 130 mm downstream from the throat of the cavitation source for the large and small working sections, respectively. The transducer was connected to a charge amplifier type (TA-3/C). The voltage output from the charge amplifier was measured using Bruel and Kjaer 1/3 octave frequency analyzer (type 2112). The sound pressure level of each 1/3 octave band from 31.5 Hz to 31.5 kHz obtained and was expressed in decibels (dB) relative to 1μ bar, that is 20 log10 (P / 1μ bar). The sound pressure levels at various frequencies were obtained at a particular cavitation number. These measurements were repeated for many other cavitation numbers and velocities.

4.2 Cavitation Inception

Prior to each series of inception measurements at a certain configuration, the tunnel was run under intense cavitation conditions for a period of about 15 minutes and the liberated air from water bled of through the vent valve (see No 11 fig. 2) to achieve equilibrium air content before each test.

The inception of cavitation was obtained visually using stroboscopic light through the Perspex transparent side of the working section. The visual observations of the flow past a cavitating source started from an arbitrary pressure in the test section in the range of 2-9 bar. The flow velocity at the th-roat was increased step by step until inception of cavitation occurred. Then the flow velocity was further increased to a maximum velocity corresponding to the breakdown condition. The measurements of pressure, temperature and flow velocity upstream of the cavitating source corresponding to inception and breakdown conditions were noted. These visual observations were repeated for many other arbitrary pressures and the corresponding readings were determined. The cavitation numbers corresponding to inception and breakdown conditions upstream of the cavitating source were obtained from the following Eqs.

$$\sigma_0 = \frac{p_0 - p_V}{0.5\rho u_o^2} \tag{5}$$

where P_0 and U_0 are respectively the pressure and velocity upstream of the source. Cavitation number corresponding to inception condition at source throat was obtained from the measured value of the upstream inception cavitation number (σ_{0i}) as follows

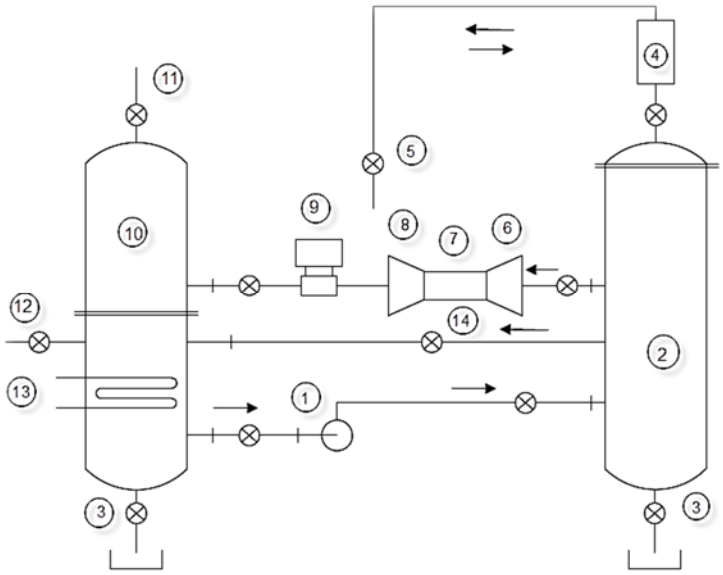

1	Centrifugal pump	8	Diffuser section
2	Upstream tank	9	Electromagnetic flow meter
3	Drain	10	Downstream tank
4	Air Vessel	11	Air vent 12- water supply
5	Compressed air supply	13	Cooling coil
6	Contraction nozzle	14	Bypass line
7	Test section 20 x 40 mm		

Fig. 2. Cavitation research water tunnel line diagram and a list of its major components.

$$\sigma_{\circ} = \frac{\sigma_{0i} - \sigma_{0b}}{1 + \sigma_{0b}} \tag{6}$$

σ_{0b} , is the value of σ_0 when the breakdown condition has been reached, p_v is the vapor pressure, at bulk temperature.

5. Analysis Of Results

5.1 Visual Observations of Inception and Breakdown Conditions

The cavitation phenomenon takes place between inception condition and breakdown condition in any system. They are very complicated and depend on so many factors. Inception means the first appearance of a cavitation zone. The breakdown condition means the cavity is very long and its walls become transparent and it appears much more stable and produces a much smaller noise level.

The average values of inception and breakdown cavitation numbers obtained by visual measurements with stroboscopic light for the six sources in both the large and small working sections are presented in Table 1.

Table 1 shows that the breakdown cavitation number σ_{0b} does not vary with source size for a given source shape. For a given source size, it may be seen that the average value of breakdown cavitation number (σ_{0b}) is higher for the forward facing step than, that for con-div wedge and the rear facing step (Table 1).

Table 1 Average visual measured values of inception and breakdown cavitation numbers for various cavitation sources

Configuration	Size (mm)	σ_{ob}	σ_{oi}	σ_i
Con-div wedge	20	4.08	8.6	0.89
	10	4.02	5.56	0.506
Rear facing step	20	3.5	6.1	0.577
	10	3.46	5.69	0.5
Forward facing step	20	8.1	14.47	0.7
	10	8.08	13.07	0.546

A significant increase of the inception cavitation number with source size in the case of con-div wedge and the forward facing step is shown in Table l. However, in the case of the rear facing step, increases of the inception cavitation number with size not appreciably. It can be seen that for a given source size, the inception cavitation number has different values depending on the shape of the cavitation source (Table l). This variation can be interpreted in terms of a change in the flow regime between one shape and another. Moreover, in a water tunnel the pressure gradient and the boundary

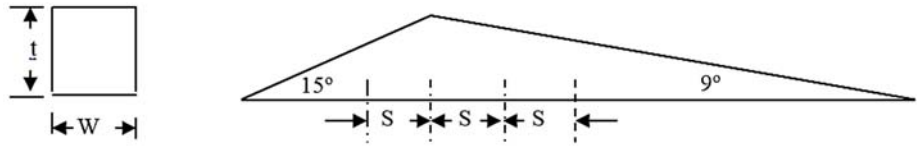

(a) Con – div wedge source.

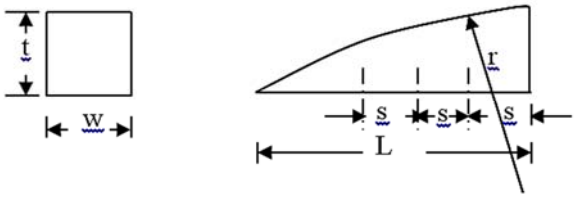

(b) Rear – facing step source.

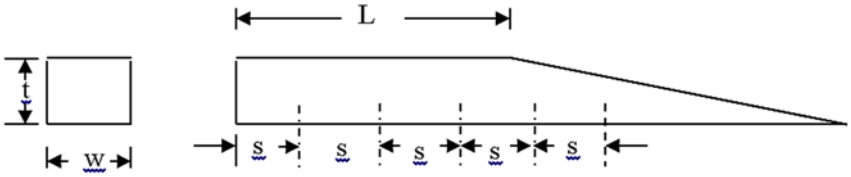

(c) Forward facing step source.

Configuration	Size (mm)	Dimension (mm)				
		t	w	s	l	r
Con-div wedge (a)	20	20	20	30	-	-
	10	10	10	15	-	-
Rear facing step (b)	20	20	20	15	72	130
	10	10	10	7.5	36	65
Forward facing step (c)	20	20	20	30	200	-
	10	10	10	15	100	-

Fig. 3. Details of cavitation sources.

layer are function of the shape of the cavitation l source and therefore every configuration wil exhibit a different value of inception cavitation number.

In order to have a qualitative clarification of the location and form of inception, the flow past the test sources was observed visually. It was observed that the inception always began at the sharp edge at the throat of the con.-div. wedge source in the form of bubbles attached to the front of divergent section of the source. For ear-facing step source the inception occurred within the wake behind the source at approximately one time the source height in the form of filament of separated bubbles. In case of forward –facing step source inception appeared as tiny bubbles attached and span wise uniformity along the entrance edge at approximately 2 mm downstream of the entrance edge of the source.

5.2 Noise level

The variation of the sound pressure level with cavitation number at frequencies above 1 kHz and at constant throat velocity of 28 m/sec is given in Figs. 4 to 9 for 20 mm con-div, 10 mm con-div, 20 mm rear facing step, 10 mm rear facing step, 20 mm forward facing step, and 10 mm forward facing step respectively. These figures show that the sound pressure level maintained nearly a constant value from higher cavitation number to a critical cavitation number at which the sound pressure level rises suddenly at frequencies above 2 kHz. Whilst at frequencies of 1 kHz and 2 kHz (i.e. low frequency noise) the sound pressure level increased as the cavitation developed. The sudden rise in the high frequency noise is about 12 dB higher than the noise level at higher cavitation number. This sudden

rise in the sound pressure level accompanies the formation of cavitation. As the cavitation number is decreased beyond the critical cavitation number, more bubbles are produced and the extent of cavitation increases with higher collapse pressure which in turn increases the radiated sound pressure level, as shown in Figs 4 to 9.

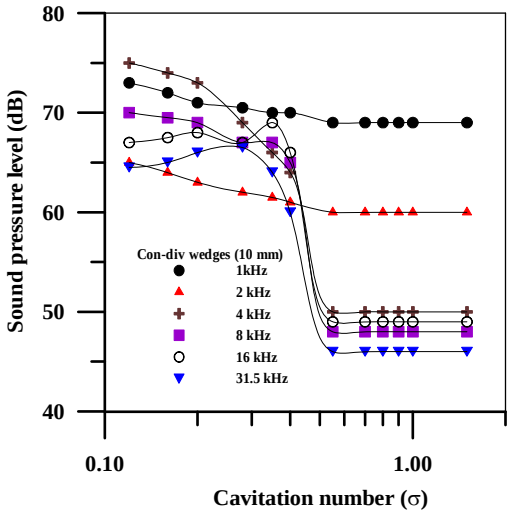

Fig. 4. Variation of sound pressure level with cavitation number at various frequencies for 10 mm con-div wedges.

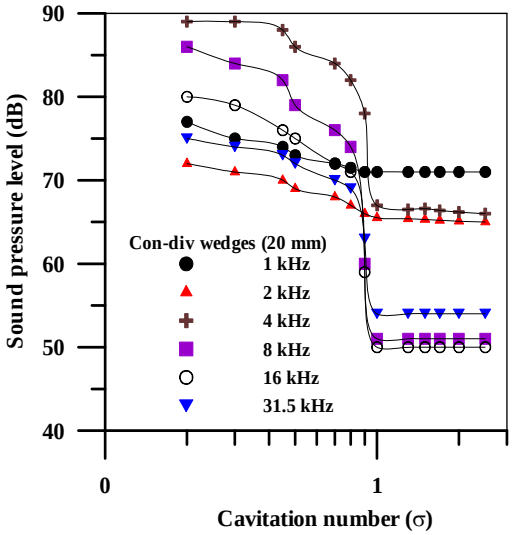

Fig. 5. Variation of sound pressure level with cavitation number at various frequencies for 20 mm con-div wedges.

Although the radiated sound is small and could not be detected by ear because of the limited size of the collapsing bubbles, the sound pressure level increases considerably at the inception of cavitation in the high frequency range as the smaller bubbles are associated with higher frequencies. It is also evident from in Figs. 4 to 9 that the point of inception occurs at the same value of cavitation number irrespective of the frequency chosen, provided it is above the critical frequency.

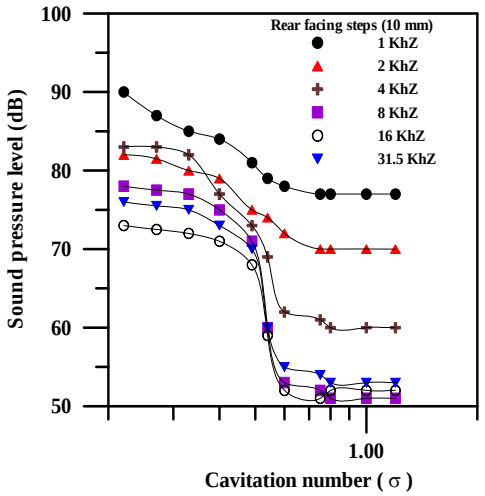

Fig. 6. Variation of sound pressure level with cavitation number at various frequencies for 10 mm rear – facing steps.

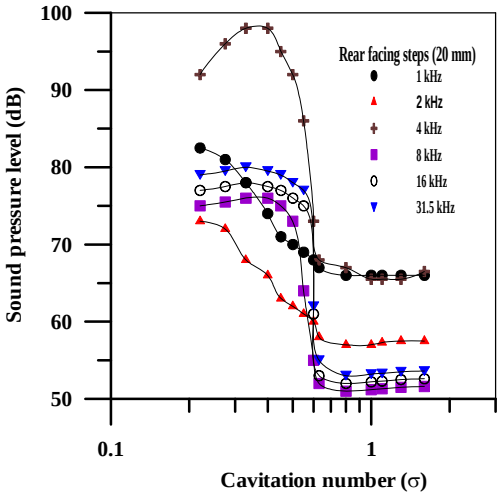

Fig. 7. Variation of sound pressure level with cavitation number at various frequencies for 20 mm rear – facing steps.

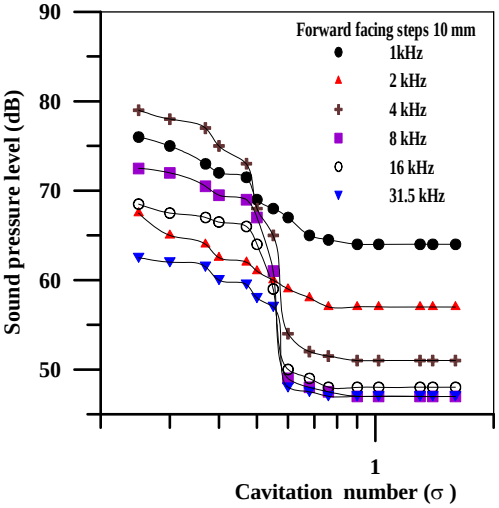

Fig. 8. Variation of sound pressure level with cavitation number at various frequencies for 10 mm forward facing steps.

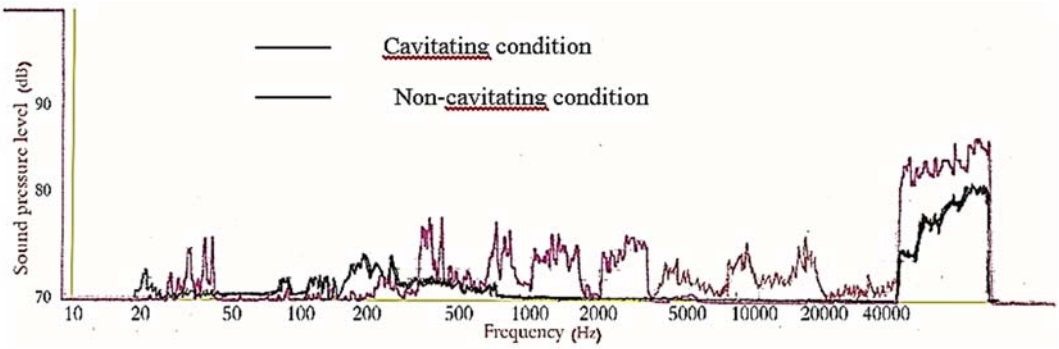

Fig. 10. Typical 1/3 octave spectra spectrograms at non-cavitating condition and cavitation inception condition for 10 mm rear- facing step at a flow velocity of 28 m/s.

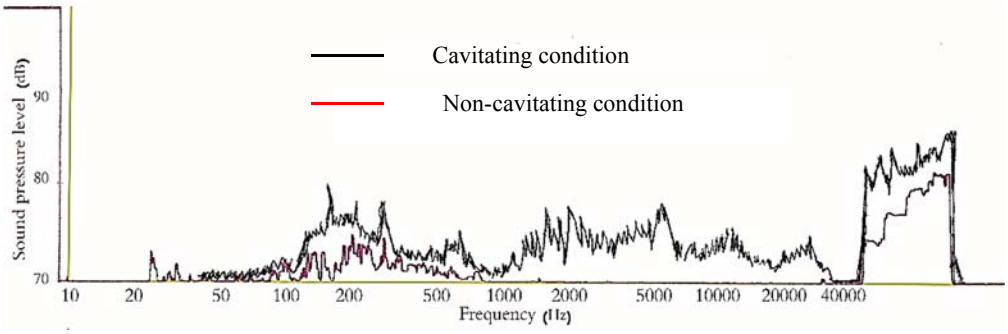

Fig. 11. Typical 1/3 octave spectra spectrograms at non-cavitating condition and cavitation inception condition for 20 mm con-div wedge at a flow velocity of 28 m/s.

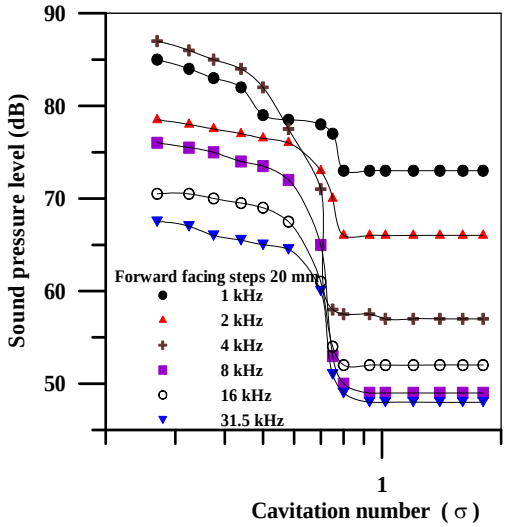

Fig. 9. Variation of sound pressure level with cavitation number at various frequencies for 20 mm forward facing steps.

A comparison of the critical cavitation number according to the noise measurements with the inception cavitation number according to visual observations, indicates that the location of points of inception obtained by visual observation lies at the sharp rise of the sound pressure level from which the point of inception could be clearly identified as shown in Figs. 4 to 9. This supported by calculating the pulsating frequency from Eqs. 1 and 4 which is presented in Fig. 1. This finding implies that measuring the sound pressure level at high frequency could be used to detect the onset of cavitation.

5.3 1/3 Octave Band Spectra

Spectra spectrograms at various cavitation numbers with a constant flow velocity and constant cavitation number and various velocities were obtained for all sources mentioned before. Fig. 10 and 11show typical 1/3 octave spectra spectrograms at non-cavitating condition and cavitation inception condition for 10 mm rear- facing step and 20 mm con-div wedge at a flow velocity of 28 m/s, respectively. In examining the corresponding results indicated in Figs. 10 and 11, an interesting variation of the spectra between non-cavitating condition and cavitation incipient condition is observed. The Fig. shows that the spectra levels for frequencies below 400 Hz are almost the same. This is possibly because for frequencies below 400 Hz the noise levels were dominated by pump rig and background noise. For frequencies more than 500 Hz the sound pressure levels increase as the onset of cavitation takes place. This means that the noise spectra corresponding the early stages of cavitation, i.e., cavitation inception (onset) contain much of the energy in the high frequencies rang. This may be attributed to the existence of a relatively large number of smaller bubbles. This finding implies that the noise measurements at higher frequencies could be used as reliable indicator for the incipient of cavitation. It is interesting to note that these

findings agreed qualitatively with the theoretical estimate of the pulsating frequency of the cavitation nuclei at various initial radius of nuclei shown in Fig. 1.

5. CONCLUSION

The noise measurements for detecting inception of cavitation are promising. It is adoptable for any flow situation, no matter where cavitation occurs. The results of the experiments indicate that inception of cavitation can be detected by an increase in the sound pressure level at any frequency above the critical frequency obtained from cavitation noise spectra. The results showed that the value of the critical frequency was 4 kHz for all cavitation sources tested. The clear and marked rise in the sound pressure level at the point of inception leads to a definite and accurate method of determining the point of inception for hydraulic machines. This finding was supported by the present theoretical estimate of the pulsating frequency of the cavitation nuclei.

REFERENCES

Al Thobiani, F., F. Gu and A. Ball (2011). Monitoring of cavitation in centrifugal pumps using a non-invasive capacitance sensor. *Proc. 24th Int. Congress on Condition Monitoringand Diagnostics Engineering Management, Stavanger, Norway.*

Alfayez, L. and D. Mba (2004). Detection of incipient cavitation and best efficiency point in a 2.2MW centrifugal pump using acoustic emission. *J. Acoustic Emission* 22, 77-82.

Alhashmi, S. A. (2005). *Detection and Diagnosis of Cavitation in Centrifugal Pumps*. Ph.D. Thesis, School of Mechanical, Aerospace and Civil Engineering, University of Manchester: Manchester.

Alhashmi, S. A. (2013). Statistical analysis of acoustic signal for cavitation detection. In *Proceeding of International Conference on Modern Trends in Science, Engineering and Technology (ICMTSET 2013),* Dubai, UAE.

Campos-Pozuelo, C., C. Granger, C. Vanhille, A. Moussatov and B. Dubus (2005). Experimental and theoretical investigation of the mean acoustic pressure in the cavitation field. *Ultrason. Sonochem.* 12(1), 79-84.

Černetič, J. and M. Čudina (2012). Cavitation noise phenomena in centrifugal pumps. *5th Congress of Alps-Adria, Acoustics ssociation, 12-14,* Petrčane, Croatia.

Černetič, J., J. Prezelj and M. Cudina (2008). Use of noise and vibration signal for detecting and monitoring of cavitation in kinetic pumps. *The Journal of the Acoustical Society of America* 123(5), 3316-3316.

Chudina, M. (2003). Noise as an indicator of cavitation in a centrifugal pump. *Acoustical Physics* 49(4), 463-474.

Čudina, M. (2012). Monitoring of cavitation by sound in audible range and some new proposals for prevention cavitation in kinetic pumps. *5th Congress of Alps-Adria Acoustics Association 12-14*, Petrčane, Croatia.

Cudina, M. and J. Prezelj (2009). Detection of cavitation in the operation of kinetic pumps: Use of discrete frequency tone in audible pump spectra using audible sound. *Applied Acoustics* 70(4), 540-564.

Franc, J. P. (2006). Physics and control of cavitation. *Physics and Control of Cavitation. Educational Notes RTO-EN-AVT-143, Paper 2, 2-1–2-36.*

Gupta, S., V.K. Chouksey, and M.Srivastava, (2013) .Online detection of cavitation phenomenon in a centrifugal pump using audible sound. *ITSI Transactions on Electrical and Electronics Engineering (ITSI-TEEE),* 1(5), 103-107.

Jensen, J. and K. Dayton (2000). Detecting cavitation in centrifugal pumps experimental results of the pump laboratory. *ORBIT Second Quarter,* 26-30.

Mostafa N., M. M. Karim and M. M. A. Sarker (2016). Numerical prediction of unsteady behavior of cavitating flow on hydrofoils using bubble dynamics cavitation model. *Journal of Applied Fluid Mechanics* 9(4), 1829-1837.

Moussatov, A., C. Granger and B. Dubus (2003-a). Cone-like bubble formation in ultrasonic cavitation field. *Ultrason. Sonochem.* 10(4), 191-195.

Moussatov, A., C. Granger and B. Dubus (2005). Ultrasonic cavitation in thin liquid layers. *Ultrasonics Sonochemistry 12, 415-422.*

Moussatov, A., R. Mettin, C. Granger, T. Tervo, B. Dubus and W. Lauterborn (2003-b). Evolution of acoustic cavitation structure near larger emitting surface. *WCU 2003, Paris, September,* 7-10, 955-958.

Park, C., H. Seol, K. Kim and W. Seong (2009). A Study on propeller noise source localization in a cavitation tunnel. *Ocean Engineering* 36-754-762.

Wu, D., L. Wang, Z. Hao, Z. Li and Z. Bao (2010). Experimental study on hydrodynamic performance of a cavitating centrifugal pump during transient operation. *Journal of Mechanical Science and Technology 24(2), 575-582.*

APPENDIX A

Details of the derivation of Eq. 1.

Consider a spherical cavity with a mean radius r0 experiencing a uniform, small harmonic fluctuation of its volume. This volume fluctuation causes a rate

of change of fluid in the medium, i.e., a mass flux, Q, which can be expressed by:

$$Q(t) = Q_0 \cos \omega t = Q_0 e^{i\omega t} \quad \text{(A1)}$$

Assume that the relative change of volume of the sphere is small, the mass flux is given by:

$$Q(t) = \rho_0 4\pi r_0^2 u \quad \text{(A2)}$$

Where ρ0 is the density of the liquid, and u is the radial velocity of the surface of the spherical cavity.

The instantaneous surface velocity is expressed by:

$$\underline{u} = u_0 e^{i\omega t} = \frac{Q_0}{4\pi r_0^2 \rho_0} e^{i\omega t} \quad \text{(A3)}$$

Since the fluid is everywhere in contact with vibratory surface of the cavity, the acoustic particle speed, $v'(r_0)$, must equal the surface vibratory speed ,u. Accordingly, the acoustic pressure at the surface of the sphere can be calculated by the following eq.:

$$\underline{p}'(r_0) = z_r(r_0) v'(r_0) = z_r(r_0) \underline{u} \quad \text{(A4)}$$

Where z_r is the specific acoustic impedance evaluated at the surface. The acoustic impedance is given by:

$$z_r = \rho_0 c_0 \frac{(kr)^2 + i(kr)}{1 + (kr)^2} \quad \text{(A5)}$$

The specific acoustic impedance is a function of relative distance because the particle speed has both near-and far-field terms.

The quantity $\rho_0 c_0$ is a property of liquid. It is called the characteristic impedance of the liquid. k is the wave number $\left(k = \frac{\omega}{c_0}\right)$.

In the near field kr < 1, the impedance is dominantly reactive; while in the far field it is basically resistive and for large kr approaches the plane-wave value.

The resistive and reactive components from a complex number which can be expressed in the exponential form,

$$z_r = \rho_0 c_0 \frac{kr}{\sqrt{1 + (kr)^2}} \cdot \frac{kr + i}{\sqrt{1 + (kr)^2}} =$$

$$\rho_0 c_0 \cos\theta (\cos\theta + i \sin\theta) = \rho_0 c_0 \cos\theta . e^{i\theta} \quad \text{(A6)}$$

Where θ is the phase angle between the pressure and the velocity on the surface of the sphere, defined by:

$$\theta = \tan^{-1}\left(\frac{1}{kr_0}\right) = \frac{\pi}{2} - \tan^{-1} kr_0 \quad \text{(A7)}$$

Combining eqs. A3, A4, A5 and A6, the pressure at distance r from the center of the sphere is,

$$\underline{p}'(r) = \frac{\omega Q_0}{4\pi r} \left(\frac{e^{i(\theta + kr_0)}}{\sqrt{1 + (kr_0)^2}} \right) e^{i(\omega t - kr)} \quad \text{(A8)}$$

At kr << 1 the term between the two brackets in eq. A8 reduces to i. therefore, the radiated pressure at distance r from the center of the spherical cavity bubble is:

$$\underline{p}'(r) = i \frac{\omega Q_0}{4\pi r} e^{i(\omega t - kr)} = -\frac{kr Q_0 C_0}{4\pi r^2} (\cos \omega t . \sin kr) \quad \text{(A9)}$$